The EMBO Journal Vol.16 No.5 pp.899–907, 1997

A mutation causing pseudohypoaldosteronism type 1 identifies a conserved glycine that is involved in the gating of the epithelial sodium channel

Stefan Gründer, Dmitri Firsov, Sue S.Chang[1], Nicole Fowler Jaeger, Ivan Gautschi, Laurent Schild, Richard P.Lifton[1] and Bernard C.Rossier[2]

Institut de Pharmacologie et de Toxicologie de l'Université, Rue du Bugnon 27, CH-1005 Lausanne, Switzerland and [1]Howard Hughes Medical Institute, Department of Medicine and Genetics, Boyer Center for Molecular Medicine, Yale University School of Medicine, New Haven, CT 06510, USA

[2]Corresponding author

S.Gründer and D.Firsov contributed equally to this work

Pseudohypoaldosteronism type 1 (PHA-1) is an inherited disease characterized by severe neonatal salt-wasting and caused by mutations in subunits of the amiloride-sensitive epithelial sodium channel (ENaC). A missense mutation (G37S) of the human ENaC β subunit that causes loss of ENaC function and PHA-1 replaces a glycine that is conserved in the N-terminus of all members of the ENaC gene family. We now report an investigation of the mechanism of channel inactivation by this mutation. Homologous mutations, introduced into α, β or γ subunits, all significantly reduce macroscopic sodium channel currents recorded in *Xenopus laevis* oocytes. Quantitative determination of the number of channel molecules present at the cell surface showed no significant differences in surface expression of mutant compared with wild-type channels. Single channel conductances and ion selectivities of the mutant channels were identical to that of wild-type. These results suggest that the decrease in macroscopic Na currents is due to a decrease in channel open probability (P_o), suggesting that mutations of a conserved glycine in the N-terminus of ENaC subunits change ENaC channel gating, which would explain the disease pathophysiology. Single channel recordings of channels containing the mutant α subunit (αG95S) directly demonstrate a striking reduction in P_o. We propose that this mutation favors a gating mode characterized by short-open and long-closed times. We suggest that determination of the gating mode of ENaC is a key regulator of channel activity.

Keywords: amiloride/channel gating/epithelial sodium channel/pseudohypoaldosteronism/salt-wasting syndrome

Introduction

The amiloride-sensitive epithelial Na channel (ENaC) is a highly selective Na channel found at the apical membrane of salt-reabsorbing tight epithelia of tissues including the distal nephron, the distal colon, the salivary and sweat glands and the lung. In these polarized epithelia, the ENaC-mediated entry of sodium into the cell represents the rate-limiting step for the vectorial movement of sodium from the mucosal to the serosal side. In the kidney, ENaC activity is controlled by aldosterone, serving to maintain salt homeostasis and blood pressure (Rossier and Palmer, 1992; Rossier *et al.*, 1994).

The primary structure of ENaC has been elucidated by functional expression cloning in *Xenopus* oocytes. It is made up of at least three homologous subunits (α, β and γENaC) which share ~35% identity in their amino acid sequences (Canessa *et al.*, 1993, 1994b). Each subunit has two transmembrane domains with short cytoplasmic N- and C-termini and a large extracellular loop (Canessa *et al.*, 1994a; Renard *et al.*, 1994; Snyder *et al.*, 1994). The biophysical properties and the pharmacological profile of ENaC expressed in *Xenopus* oocytes are similar to those for the native channel in the distal nephron (Palmer and Frindt, 1986; Canessa *et al.*, 1994b).

The importance of ENaC for the regulation of sodium balance, blood volume and blood pressure has been demonstrated by the finding of mutations in either the β or the γ subunits that cause increased ENaC activity and Liddle's disease, a rare, inherited form of salt-sensitive hypertension (Shimkets *et al.*, 1994; Hansson *et al.*, 1995). Recently, it has been shown that pseudohypoaldosteronism type 1 (PHA-1), an inherited disease characterized by severe neonatal salt-wasting, hyperkalaemia, metabolic acidosis and unresponsiveness to mineralocorticoid hormones, is also caused by mutations in ENaC subunits (Chang *et al.*, 1996), further confirming the important role of ENaC for salt and water homeostasis. These mutations lead either to a frameshift or a premature stop codon in the α subunit or to an amino acid exchange in a conserved region at the N-terminus of the β subunit (Chang *et al.*, 1996). The functional consequences of this mutation in the β subunit (G37S) were investigated by co-expression of the βG37S subunit with wild-type α and γ subunits in *Xenopus* oocytes. Oocytes expressing mutant channels showed an ENaC activity which was reduced to ~40% of the activity of oocytes expressing wild-type channels. Oocytes expressing the mutant β subunit, however, still had significantly higher activity than oocytes expressing only α and γ subunits (Chang *et al.*, 1996). This finding demonstrated that this mutation does not result in complete loss of function, leaving unresolved the mechanism by which this mutation leads to a reduction in ENaC activity. Here we report that introduction of the homologous mutation into the α subunit (αG95S) drastically reduces the open probability (P_o) of the single channel, suggesting that the N-terminal domain containing the conserved glycine controls the gating of ENaC.

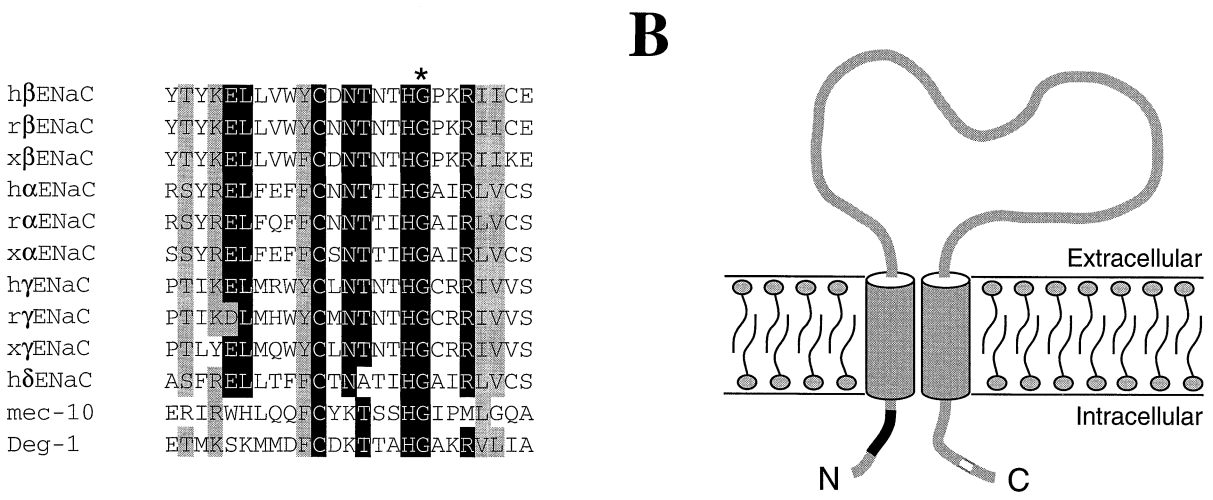

Fig. 1. (**A**) N-terminal amino acid sequence of different homologs of the ENaC gene family. Sequences have been aligned so as to show maximal homology. Amino acids showing a high degree of identity are shown as white letters on a black background, those showing a high degree of homology as black letters on a gray background. The prefixes h, r and x denote genes from human (McDonald *et al.*, 1994, 1995; Waldmann *et al.*, 1995), rat (Canessa *et al.*, 1993, 1994b) and *X.laevis* (Puoti *et al.*, 1995), respectively. mec-10 and Deg-1 are homologs from *Caenorhabditis elegans* (Chalfie and Wolinsky, 1990; Chalfie *et al.*, 1993; Huang and Chalfie, 1994). The glycine at position 37 of hβENaC which is mutated to serine in PHA-1 is marked by an asterisk. (**B**) Model of the transmembrane topology of ENaC subunits. The N-terminal domain shown in (A) is highlighted in black, the PY motif involved in Liddle's disease in white.

Results

Macroscopic amiloride-sensitive sodium currents of the G37S mutation in βENaC and of the corresponding mutations in α and γENaC

Gly37 of βENaC is conserved in all known subunits of this gene family and is located in a highly conserved stretch of ~20 amino acids (Figure 1A) preceding the first transmembrane-spanning region (Figure 1B). According to the established ENaC membrane topology, this N-terminal segment is facing the cytoplasmic side of the membrane (Canessa *et al.*, 1994a; Renard *et al.*, 1994; Snyder *et al.*, 1994). As the overall homology between different ENaC subunits is low (30–35% at the amino acid level), the high degree of identity of the segment containing Gly37 suggests an important role for normal ENaC function. Elucidation of the mechanism by which the Gly37→Ser (G37S) mutation decreases ENaC activity could thus help to define the role of this domain.

Gly→Ser mutations were introduced at homologous positions in α, β and γENaC. As an index of ENaC channel activity, we measured the macroscopic amiloride-sensitive Na^+ current (I_{Na}). As shown in Figure 2A a highly significant decrease in ENaC activity was seen with the three mutants. αG95S showed the most drastic effect, reducing I_{Na} to ~15% of wild-type activity ($P < 0.001$); γG40S reduced I_{Na} to ~55% ($P < 0.001$), similar to the effect of βG37S (62% of wild-type activity; $P < 0.02$). Thus, the conserved Gly residue of all three subunits is essential for normal channel activity. Co-expression of more than one mutant subunit resulted in a cumulative effect. When βG37S was co-injected with γG40S, ENaC activity decreased to 11% of wild-type activity ($P < 0.001$, Figure 2B) and co-expression of three mutant subunits (αG95SβG37SγG40S) resulted in a complete loss of ENaC activity ($P < 0.001$, Figure 2B).

As the measure of I_{Na} would be invalid if the mutations changed the affinity of the channel for amiloride, we verified for the βG37S and the αG95S mutant subunits that these point mutations do not change the affinity of ENaC for amiloride (data not shown).

I_{Na} depends on several variables given by the following relationship:

$$I_{Na} = g_{Na} N P_o (E–E_{Na}) \qquad \text{(Equation 1)}$$

where g_{Na} is the unit conductance for a single ENaC channel, N is the number of conductive ENaCs per unit area of membrane, P_o is the open probability of a single ENaC, E is the membrane potential and E_{Na} is the reversal potential for sodium. To keep the driving force for the sodium ion ($E – E_{Na}$) in our whole cell experiments largely constant, we always strongly hyperpolarized the oocyte membrane to –100 mV. Moreover, we observed that oocytes expressing ENaC wild-type channels had a significantly more depolarized resting potential [–15.7 ± 1.6 mV (mean ± SEM), $n = 78$] than oocytes expressing mutant βG37S channels [–28.9 ± 1.8 mV (mean ± SEM), $n = 84$, $P < 0.001$]. This observation suggests that βG37S ENaC mutants were less charged with sodium than oocytes expressing wild-type ENaC, consistent with the observed reduction of channel activity. This would tend to increase the driving force for Na entering the cell (thus I_{Na}) and cannot account for the observed decrease in I_{Na} with mutant ENaC. Therefore, the decrease in I_{Na} caused by Gly→Ser mutations can either involve a change in single channel conductance reflecting an impaired permeation of Na^+ ions through the channel, a decrease in channel open probability, or fewer channels expressed at the cell surface. The later decrease in cell surface expression of channel mutants can be related either to a misassembly of channel subunits or to a defective targeting of the ENaC channel to the cell surface.

Synthesis and assembly of mutant subunits

The highest degree of homology within the region containing Gly37 is found between αENaC and a recently

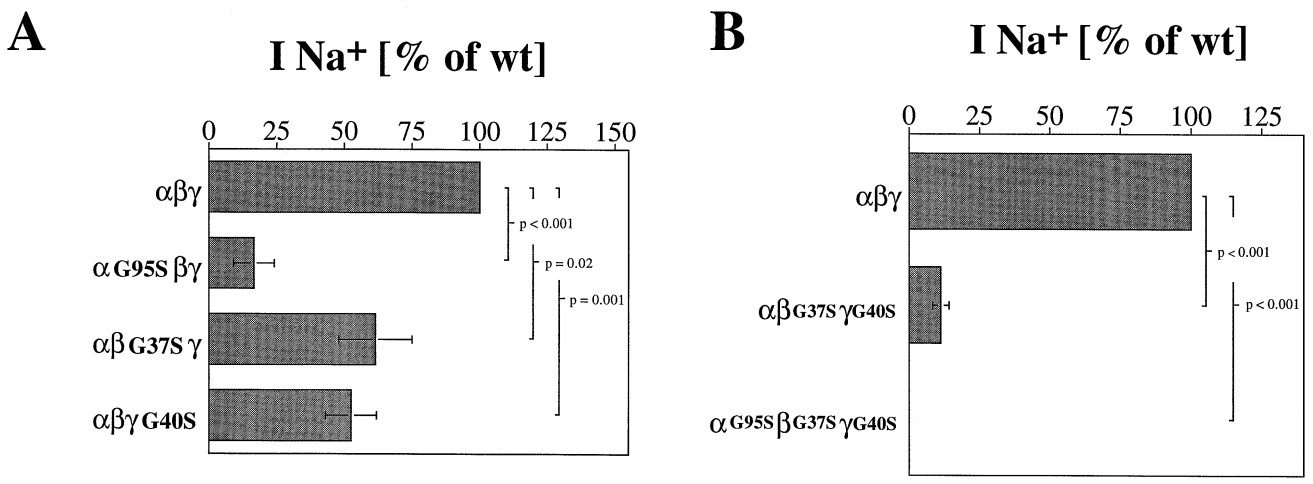

Fig. 2. Effects of glycine to serine substitutions in α, β and γENaC on amiloride-sensitive (5 μM) sodium current (I_{Na}). (**A**) Glycine homologous to Gly37 of the β subunit was replaced by a serine in α and γ subunits. cRNAs encoding either one of the three mutant subunits (αG95S, βG37S, γG40S) were co-injected with two wild-type subunits as indicated. Oocytes injected with three wild-type subunits served as a control. The activity of mutant channels is represented as the I_{Na} normalized for the activity of wild-type channels. Macroscopic I_{Na} for wild-type ENaC was 11.12 ± 4.30 μA (n = 5). Holding potential was –100 mV. (**B**) cRNAs encoding either three wild-type subunits, wild-type α with mutant β and γ subunit or three mutant subunits were co-injected. Macroscopic I_{Na} for wild-type ENaC was 2.32 ± 0.05 μA and for the αG95SβG37SγG40S mutant channel 1 ± 0.5 nA (n = 4). The difference in activity was also highly significant for individual oocytes (P <0.001). Holding potential was –100 mV. Bars represent the I_{Na} normalized for the wild-type activity, error bars the SEM. P-values for t-tests comparing mutant and wild-type activity are indicated.

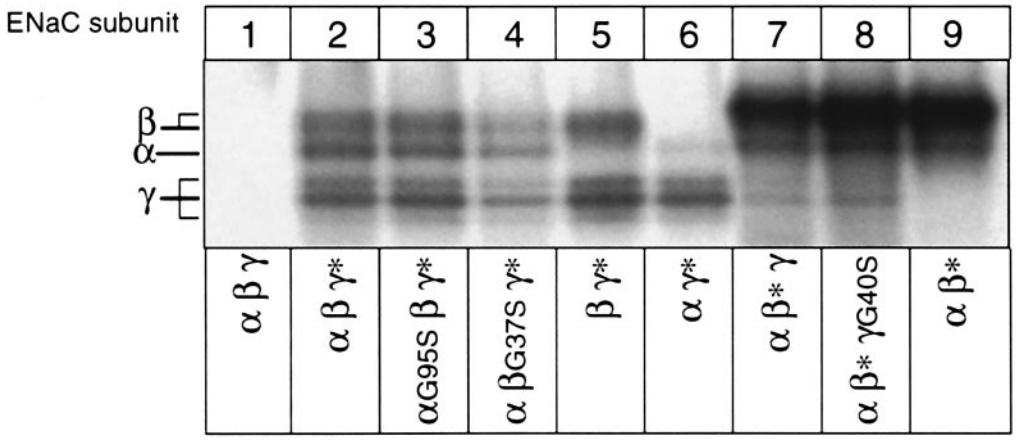

Fig. 3. Co-immunoprecipitation of wild-type and mutant ENaC subunits. Oocytes were either injected with three untagged wild-type subunits (lane 1) or with an epitope (FLAG)-tagged β or γ wild-type subunit (marked by an asterisk) co-injected with one or two wild-type or one wild-type and one mutant subunit (lanes 2–9). Anti-FLAG monoclonal antibodies were used to immunoprecipitate tagged β or γENaC, and associated subunits were co-immunoprecipitated under non-denaturing conditions. The specificity of the monoclonal antibody is shown in lane 1 (no tagged subunit) and the specificity of the co-immunoprecipitation in lanes 5, 6 and 9 (either one of the three subunits is missing).

cloned new member of this gene family, δENaC (Figure 1A), both of which are characterized by their ability to associate with β and γ subunits and to enhance ENaC activity (Canessa *et al.*, 1994b; Waldmann *et al.*, 1995), raising the possibility that this domain is involved in the assembly of ENaC subunits.

To assess the proper association of ENaC subunits, we used an epitope (FLAG)-tagged β or γ subunit to immunoprecipitate, with an anti-FLAG monoclonal antibody, the αβγENaC complex from microsomes prepared from ^{35}S metabolically labeled ENaC-expressing oocytes. As shown in Figure 3, anti-FLAG antibodies do not immunoprecipitate proteins from oocytes expressing three untagged ENaC subunits (Figure 3, lane 1). When one of the subunits (β or γ) carried the FLAG epitope, we co-immunoprecipitated three predominant proteins from oocytes expressing α, β and γENaC (Figure 3, lanes 2 and 7). These proteins correspond to α, β and γENaC as previously shown in immunoprecipitations using antisera specific for each of these proteins (Duc *et al.*, 1994). As unassembled epitope-tagged subunits will also be immunoprecipitated, greater amounts of immunoprecipitated tagged βENaC as compared with tagged γENaC are probably due to a more efficient translation of βENaC in *Xenopus* oocytes. From oocytes injected with only two subunits we precipitated only two of the predominant proteins, demonstrating the specificity of the co-immunoprecipitation (Figure 3, lanes 5, 6 and 9). From oocytes expressing one of the mutant subunits (αG95S, βG37S or γG40S) together with two wild-type subunits, one of

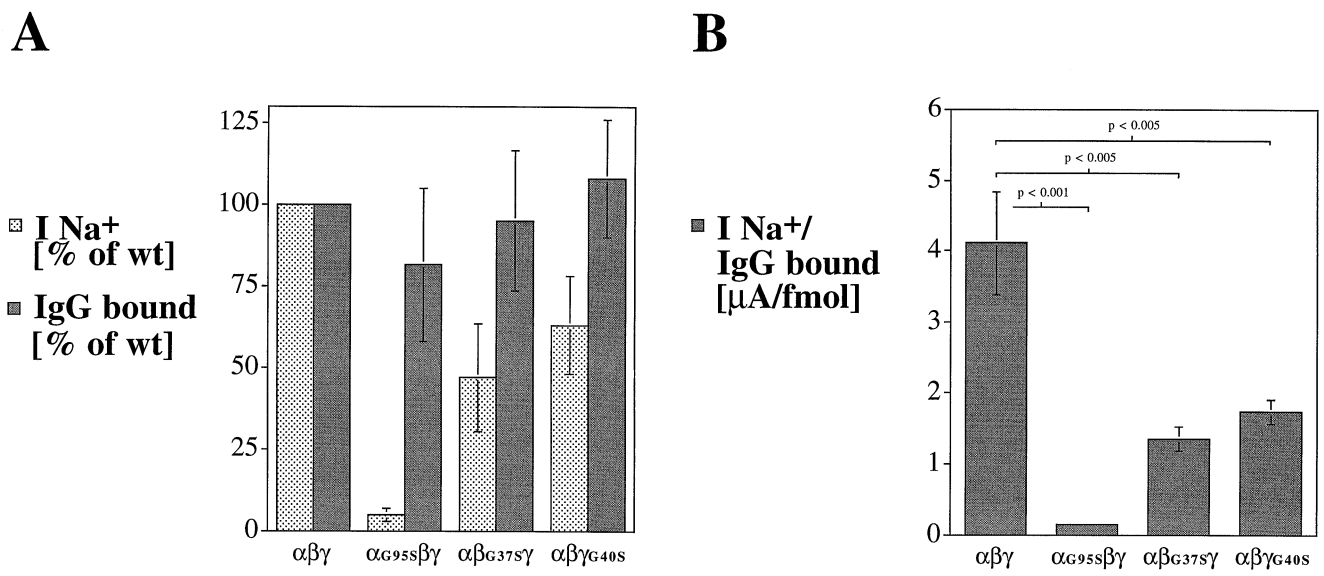

Fig. 4. Effects of glycine to serine substitutions on ENaC cell surface expression and amiloride-sensitive sodium current (I_{Na}). cRNAs encoding either one of the three mutant subunits (αG95S, βG37S, γG40S) were co-injected with two wild-type subunits as indicated. Oocytes injected with three wild-type subunits served as a control. In each of the conditions, the α and β subunit were tagged by an epitope for the anti-FLAG monoclonal antibody. ENaC expression at the surface of oocytes was determined with a ^{125}I-labeled anti-FLAG antibody. Specific binding of the antibody to mutant channels is represented as the IgG bound normalized for the binding to wild-type channels (light bars). Error bars represent the SEM. Anti-FLAG IgG bound to wild-type ENaC was 1.05 ± 0.19 femtomol (n = 6). I_{Na} has been determined from the same oocytes; it is represented as the I_{Na} normalized for the activity of wild-type channels (gray bars). Error bars represent the SEM. For all the mutants, reduction in activity was statistically significant (P <0.05). Macroscopic I_{Na} for wild-type ENaC was 3.93 ± 1.46 μA (n = 6). (**B**) Effects of glycine to serine substitutions on the ratio of the whole-cell sodium current to the bound anti-FLAG IgG. Shown are the means of the values of individual oocytes used in the experiments reported in (A). Error bars represent the SEM. P-values for t-tests comparing the ratios for mutants and wild-type are indicated.

which was epitope tagged, we co-immunoprecipitated all three predominant proteins (Figure 3, lanes 3, 4 and 8). This shows that the Gly→Ser mutation does not inhibit the association of a mutant subunit with the two wild-type subunits and the formation of a heteromultimeric αβγENaC channel. Thus, the decrease in I_{Na} resulting from expression of Gly→Ser mutant subunits with wild-type subunits does not result from the activity of ENaC channels containing only two subunits (αβ or αγ) which are characterized by a low level of amiloride-sensitive current. Moreover, since similar amounts of channel subunits are co-immunoprecipitated from oocytes expressing wild-type and mutant channels (Figure 3), it is unlikely that altered ENaC assembly accounts for the loss of channel function caused by these mutations.

Cell surface expression of mutant channels

To determine if the decrease in I_{Na} is due to a lower number of ENaC channel molecules expressed at the cell surface, we used a quantitative assay based on the binding of an [^{125}I]IgG anti-FLAG monoclonal antibody directed against a FLAG epitope in the extracellular loop of the α and the β subunit. We have demonstrated that the introduction of the FLAG epitope in the proximal part of the extracellular loop of ENaC subunits does not change the physiological and pharmacological properties of the channel (Firsov *et al.*, 1996). To compare cell surface expression directly with activity of ENaC, we first determined the specific [^{125}I]IgG anti-FLAG binding and we then measured the I_{Na} of the same oocytes.

As shown in Figure 4, mutant ENaC bearing the FLAG epitope on the α and β subunit showed I_{Na} indistinguishable from that found in channels not containing a FLAG epitope (Figure 2A) (5% of wild-type activity for αG95S, P <0.001, 47% for βG37S, P = 0.009, and 63% for γG40S, P = 0.03). In addition, the absolute values for I_{Na} (μA/oocyte) were similar to those measured without tagged subunits. In contrast to the reduced I_{Na} of mutant channels, there was no significant reduction in the number of mutant channels at the cell surface, as reflected in quantitation of specific binding of anti-FLAG IgG to channels carrying the Gly→Ser mutations in either the α, β or γ subunit. The mean of specific anti-FLAG binding sites per oocyte ranged from 0.7 to 1.05 fmol/oocyte (Figure 4). This finding indicates that the observed reduction in I_{Na} resulting from these mutations must result from reduced sodium current per channel molecule present at the cell surface. This is best illustrated (Figure 4B) by the striking decrease in the ratio of the whole cell Na^+ current (I_{Na}) to the bound anti-FLAG IgG; the mean of this ratio for individual oocytes was 4.11 μA/fmol for the ENaC wild-type, 0.15 μA/fmol for the αG95S (P <0.001), and 1.35 and 1.73 μA/fmol (P <0.005) for the βG37S and the γG40S, respectively.

Thus, the Gly→Ser mutations impair neither the assembly of ENaC subunits in a heteromeric channel nor the trafficking and expression of ENaC at the cell surface. This suggests that these mutations lead to an intrinsic channel dysfunction characterized by a reduction of the average Na^+ current passing through channels present at the cell surface. As shown by Equation 1, these mutations can decrease the macroscopic sodium currents by reducing either the single channel conductance or the probability of the channel being in the open conformation. To distinguish

between these possibilities, we analyzed the properties of single channels by measuring microscopic sodium current by patch–clamp.

Microscopic sodium currents: single channel properties of wild-type versus mutant ENaC (βG37S and αG95S)

Single channel currents were obtained in cell-attached patch configuration from oocytes expressing either ENaC wild-type, or ENaC containing either βG37S or αG95S. For the wild-type and mutants, the currents resulting from channel openings are in the pA range and the current–voltage relationship of the βG37S mutant shows the characteristic higher permeability for Li^+ over Na^+ as observed for the wild-type channel (Canessa *et al.*, 1994b). The single channel conductance of the βG37S mutant was 5 pS in the presence of Na^+ ions and 7.5 pS for Li^+ ions, values similar to those measured for the ENaC wild-type expressed in *Xenopus* oocytes. Considering that the corresponding mutation in the α subunit also exhibits a similar high conductance for Li^+ ions (g_{Li} = 6.9 pS), these single channel data indicate that the channel's ionic conductance and selectivity are not altered by the Gly→Ser mutations. From these experiments, we conclude that the glycine mutation must alter the open probability of the channel.

The single channel recording of wild-type ENaC shows long lasting opening and closing events whose duration exceed 1 s, interrupted by short closures or openings lasting <1 s. The average open probability of ENaC wild-type is ~0.5 but, as has been shown in the native tissue, this open probability is quite variable from channel to channel, ranging from 0.05 to 0.9. The individual values are not distributed normally but are mainly <0.25 or >0.75 (Palmer and Frindt, 1996). The gating behavior of wild-type ENaC was interpreted as showing two different transitions between open and closed states (Palmer and Frindt, 1996). The recording of the αG95S mutant shows characteristics different from the gating behavior of the ENaC wild-type: this mutant channel spends most of its time in the closed conformation, and the long closing events are interrupted by short duration opening events. The open probability of the αG95S mutant was significantly reduced to 0.04 ± 0.012 (mean ± SD, n = 14, P <0.001) compared with wild-type [P_o = 0.48 ± 0.26 (mean ± SD), n = 33, see Schild *et al.*, 1995]. Kinetic analysis of channel recordings showed that the mean open time duration of the opening events averaged 74 ± 54 ms (mean ± SD, n = 14); during these channel recordings (up to 15 min), no single opening event lasting >1 s could be observed. Thus, the αG95S mutation affects channel gating in which the channel mutant opens for only a short period of time, as if the mutation renders the open conformation of the channel unstable compared with ENaC wild-type.

Single channel recording of the βG37S mutant was not statistically different from wild-type, exhibiting similar long and short transitions between open and closed states, with a P_o of 0.58 ± 0.26 (mean ± SD, n = 7). A 40–50% decrease in whole-cell I_{Na} measured for the β or γ mutant channels should correspond to a P_o of 0.25–0.3, a difference from wild-type channels that cannot be detected statistically (see Discussion).

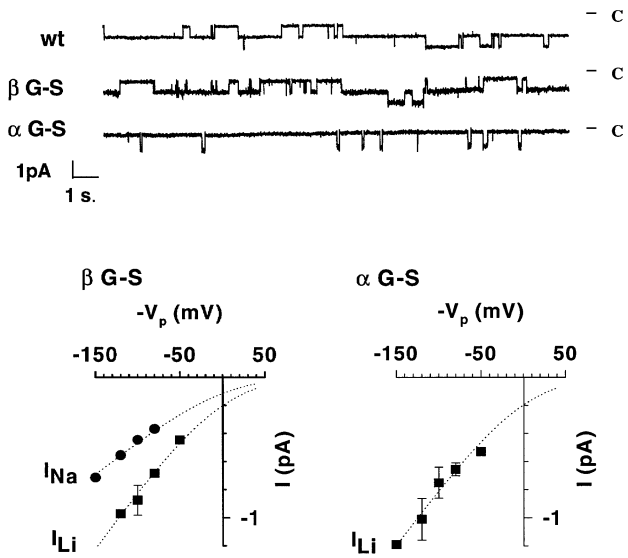

Fig. 5. Effects of G→S mutations in the α and β subunits on single channel properties. Upper panel: comparative channel recordings of αβγ ENaC wild-type, αG95Sβγ and αβG37Sγ mutants. Downward deflections represent channel openings. The pipet was filled with Li^+ as the major cation. Lower panels show current–voltage relationships of the αG95Sβγ mutant (n = 14) and αβG37Sγ mutant (n = 7). Chord conductance estimated from linear regression analysis of I_{Na} values between –50 and –150 mV was 5 and 7.5 pS for βG37S in the presenceof Na^+ and Li^+ ions respectively, and 6.9 pS for αG95S in the presence of Li^+ ions. Dotted lines represent fit to constant field equation.

The G37S mutation does not act via the phosphorylation of a PKC site created de novo by the mutation

The serine replacing the glycine generates in all the three mutant subunits a site (SXXR, Figure 1A) which could potentially be phosphorylated by protein kinase C (PKC) and consequently modify the channel open probability. To address this question, different amino acid substitutions of Gly37 of the β subunit were performed: (i) a conservative alanine substitution, (ii) a cysteine substitution that resembles the serine but is not amenable to phosphorylation, and (iii) an aspartate substitution mimicking a constitutive phosphorylation by introduction of a negative charge at this position. As shown in Figure 6, the introduction of the cysteine and the aspartate, but not of the alanine, resulted in a significant decrease in I_{Na} (65 and 1% of wild-type activity, respectively). As the reduction of I_{Na} in oocytes expressing G37C was comparable with that in oocytes expressing G37S (57% of wild-type activity), phosphorylation of Ser37 is unlikely to account for the observed decrease in channel activity. This was supported further by the observation that neither stimulation of PKC by phorbol 12-myristate-13-acetate (PMA) nor indirect stimulation of protein kinase A (PKA) by IBMX or forskolin changed I_{Na} differentially in oocytes expressing either βG37S mutant or ENaC wild-type (data not shown). The differential effect of our amino acid substitutions at codon 37 on channel function suggests that rather than abnormal phosphorylation, steric effects on the protein structure induced by mutations at position 37 are involved in the abnormal function of the channel.

Discussion

Mutations of a conserved glycine in the N-terminus of ENaC subunits that affect channel gating and explain disease pathophysiology

In order to investigate systematically by which mechanism a mutant Gly→Ser subunit present in the αβγENaC complex reduces I_{Na}, we have, according to Equation 1, measured I_{Na}, g_{Na} and N. As discussed above, a change in the driving force (E–E_{Na}) does not account for the observed decrease in I_{Na}. The results of our measurements of macroscopic sodium currents, I_{Na}, and the number N of expressed ENaCs on the same oocyte as well as the results of our measurements of g_{Na} are summarized in Table I. According to Equation 1, it is possible to deduce from this relative values for P_o. This demonstrates a significant reduction of P_o for the mutant α as well as the mutant β subunit (Table I).

A drastic reduction in the open probability (P_o = 0.04) could also be demonstrated directly for the mutant α subunit. This reduction in P_o was accompanied by a reduction in the mean open time duration, which was >1 s for the ENaC wild-type versus 74 ± 54 ms for the αG95S mutant. This 10-fold decrease in the P_o and the mean open time duration could account for the ~10-fold reduction of I_{Na} found in whole-cell voltage clamp experiments. For the mutant β subunit, we could not demonstrate directly the expected ≈2-fold decrease in P_o. This is not surprising because the gating behavior shows a large variation between channels, and channels present in the membrane patch represent only a small fraction of the channels present at the cell surface. Moreover, the measurement of P_o by patch–clamp critically depends on the confidence with which the number of channels present in the patch can be determined. As accurate assessment of this number is unfortunately impossible; the P_o as inferred from patch–clamp can only be an estimation. In contrast, with our macroscopic binding assay, we quantify the total number N of channels independently of their function. Therefore, we conclude that it is very likely that the corresponding mutation in the β subunit—like the α subunit—also reduces P_o. Our findings suggest that mutation of a conserved glycine residue in the N-terminus of ENaC subunits changes ENaC gating and that this change in ENaC gating accounts for the reduced ENaC activity causing PHA-1.

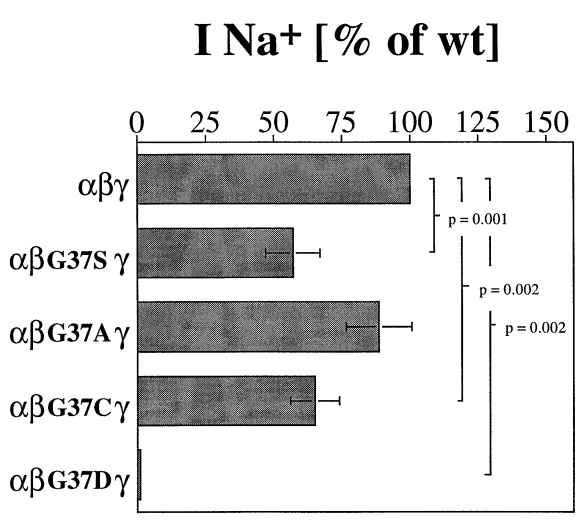

Fig. 6. Effects of amino acid substitutions at Gly37 of βENaC on the amiloride-sensitive Na current (I_{Na}). cRNAs encoding wild-type and mutant βENaC were co-injected with wild-type α and γENaC. The corresponding bars indicate the I_{Na} normalized for wild-type ENaC values; error bars represent the SEM. The *P*-values for *t*-tests comparing the activity of mutant and wild-type channels are indicated. Macroscopic I_{Na} for wild-type ENaC was 15.28 ± 5.90 μA (n = 7). Holding potential was –100 mV.

ENaC gating modes: αG95S mutant favors a gating mode showing short open and long closed times

The gating of ENaC is a complex molecular phenomenon which still remains poorly understood. This complexity is illustrated in Figure 5, where channel recordings show the presence of multiple channels and opening and closing events of variable duration. In general, channels that can be observed in membrane patches exhibit long openings and long closures with dwell times in the second range interrupted by shorter events lasting 10 to several hundred milliseconds. Such a complex gating pattern is likely to be responsible for the highly variable open probability measured for ENaC. The P_o as well as the mean open and closed times as inferred from patch–clamp studies represent, in general, the mean of many different channels present in the same patch; the values for individual channels are very difficult to determine.

A refinement of our understanding of ENaC gating comes, therefore, from a recent study in native tissue. Palmer and Frindt (1996) analysed 19 patches collected over 4 years which contained individual ENaC channels. They identified at least two different gating 'modes', one with a low open probability P_o<0.25 characterized by long closing events and short openings and the other one with a high P_o>0.75 showing long openings and short

Table I. Comparison of fractional whole cell P_o [P_o(whole cell)] versus P_o determined in cell-attached patch [P_o (patch)]

	αβγ	αG95Sβγ	αβG37Sγ	αβγG40S
I_{Na}/I_{Na} wt	1	0.05	0.47	0.63
N/N wt	1	0.81	0.95	1.08
g_{Na}	Na: 4.6 pS	Na: n.d.	Na: 5 pS	n.d.
	Li: 7.7 pS	Li: 6.9 pS	Li: 7.5 pS	n.d.
P_o (whole cell)	1	0.07	0.5	–
P_o (patch)	0.48	0.04	0.58	n.d.

I_{Na} is the whole cell amiloride-sensitive sodium current, N is the total number of ENaC expressed on the cell surface and g_{Na} is the single channel conductance. Values for I_{Na} and N are taken from Figure 4A and are normalized for wild-type; values for g_{Na} are taken from Figure 5 (αG95Sβγ, αβG37Sγ) or from Canessa *et al.* (1994b) (αβγ). The fractional whole cell P_o [P_o (whole cell)] is the ratio of the fractional values of $I_{Na}/N \times g_{Na}$. Values for P_o determined by patch–clamp [P_o (patch)] are from Figure 5. n.d., not determined.

closures. The cellular or molecular factors that determine the mode in which the channel is gating or regulate transitions between the different gating modes are not yet understood.

We recently have been able to correlate in individual oocytes the number of ENaC subunits expressed at the cell surface with the measured amiloride-sensitive Na^+ current (Firsov *et al.*, 1996). This correlation shows that the overall open probability of the channels expressed at the cell surface is <0.05, which means that the channels exhibiting a P_o of 0.25 or higher represent only a small fraction of the ENaC pool at the cell surface. The predominant pool of ENaC expressed at the cell surface with a very low P_o will escape detection in standard patch–clamp experiments.

In the context of our present knowledge of ENaC gating, how can we interpret the changes in P_o induced by the G→S mutations? The low open probability P_o and the short open dwell time duration and the long closing events characterizing the αG95S mutant are reminiscent of the low P_o gating mode described for the ENaC wild-type channels. For example, one of the channels reported by Palmer and Frindt (1996) had a P_o of 0.093 and a mean open time of 77 ms, similar to the mean values for the αG95S mutant. This observation suggests that the G→S mutation might shift the equilibrium between two normal alternative gating modes, favoring a mode with short open times and long closed times. The fact that we never observed long openings in recording of αG95S mutant channels suggests that the αG95S cannot escape the low P_o gating mode whereas the βG37S can. As the glycine is not only conserved between all the subunits of the ENaC gene family but is also located in a highly conserved segment at the intracellular N-terminus of ENaC subunits, it is tempting to speculate that this segment is involved in the normal gating of ENaCs. Mutating the conserved glycine would thus impair the normal functioning of this 'gating domain', thereby changing the equilibrium between different gating modes.

Different gating modes of ENaC: physiological importance for aldosterone regulation of channel activity

The different gating 'modes' of ENaC may have a physiological significance. The mineralocorticoid aldosterone is known to increase the activity of the epithelial sodium channel in most salt-reabsorbing tight epithelia. The mechanism by which aldosterone regulates ENaC activity is, however, still controversial. In a study investigating the effect of aldosterone on single channel characteristics of ENaC in the aldosterone-responsive epithelial cell line A6 (Kemendy *et al.*, 1992), the authors found a reduction of P_o and the mean open time of ENaCs as cells were depleted of aldosterone, suggesting that the hormone regulates ENaC activity by changing its single channel characteristics. The mean open time changed from 1615 ± 224 ms to 40.6 ms as cells were deprived for 36–72 h of aldosterone; the mean closed time changed only slightly, if at all (Kemendy *et al.*, 1992). This shows that one of the mechanisms by which aldosterone regulates ENaC activity might be by shifting channels already present at the apical membrane of epithelial cells in a different gating 'mode'. As the mean open time of ENaC of A6 cells stimulated by aldosterone resembles the mean open time of wild-type ENaC expressed in *Xenopus* oocytes (>1 s), whereas the mean open time of ENaC of A6 cells deprived of aldosterone resembles that of the αG95S mutant (74 ± 54 ms), it seems possible that the segment containing the conserved glycine is not only involved in the gating of ENaC but is also part of a functional domain of ENaC directly or indirectly regulated by aldosterone. Assuming that the G37S mutation in the β subunit also changes the equilibrium between gating modes of ENaC channels, this would explain why PHA-1 patients with this mutation do not respond appropriately to their elevated plasma aldosterone.

Mutations in ENaC subunits either reduce or increase ENaC activity causing human genetic diseases, which underscores its biological importance in sodium balance and in the control of blood pressure

Mutations found in ENaC subunits provoking genetic diseases have underscored the importance of the amiloride-sensitive sodium channel for salt and water homeostasis. These are mutations leading either to a gain-of-function characterized by increased sodium reabsorption in the distal nephron leading to Liddle's disease (Shimkets *et al.*, 1994) or to a loss-of-function characterized by a decreased sodium reabsorption in the distal nephron leading to PHA-1 (Chang *et al.*, 1996). As can be expected, gain-of-function mutations are operating on a specialized mechanism and, therefore, are limited to a defined region; in the case of Liddle's disease the C-terminus (Figure 1B) of the β and γ subunits (Shimkets *et al.*, 1994; Hansson *et al.*, 1995; Schild *et al.*, 1995; Tamura *et al.*, 1996). In contrast, loss-of-function mutations can, in principle, operate on any mechanism disturbing normal channel function and are, therefore, expected to be much more heterogeneous. In the case of PHA-1, they lead either to a disruption of the protein structure of the α subunit (Chang *et al.*, 1996) or, by the exchange of a conserved glycine in the β subunit (as we have shown in this report), very likely to the impairment of channel gating. The mechanisms involved in the other PHA-1 pedigrees are not yet known, but are probably quite different from the mechanism reported here. The two mutations reported for the α subunit lead either to a frameshift prior to the putative first transmembrane domain or to a premature stop codon in the extracellular loop prior to the putative second transmembrane domain (Chang *et al.*, 1996). As the α subunit is required for ENaC activity (Canessa *et al.*, 1993), it is likely that the frameshift mutation (I68frameshift), which results in an α subunit containing only the intracellular N-terminus, leads to a non-functional channel protein. The premature stop codon in the extracellular loop (R508stop) results in a protein containing the intracellular N-terminus, the first transmembrane domain and most of the extracellular loop, but lacks the second transmembrane domain and the intracellular C-terminus. It thus resembles two alternative splice products of the α subunit which have been identified in rat taste tissue and which delete part of the coding sequence thereby introducing premature stop codons ~50 amino acids upstream of the stop codon at position 508 (Li *et al.*, 1995). Co-expression of these alternative splice products

with wild-type β and γENaC in *Xenopus* oocytes did not induce amiloride-sensitive sodium currents (Li *et al.*, 1995), suggesting that the R508stop mutation also results in an inactive channel protein.

In a recent report (Strautnieks *et al.*, 1996), another mutation leading to PHA-1 has been identified in γENaC, introducing a splice site mutation which leads either to a disrupted protein structure or to the exchange of three highly conserved amino acids by a new one. The functional consequences of this mutation have not been reported so far, but it seems likely that it will also reduce ENaC activity. In spite of this heterogeneity of loss-of-function mutations, they might—as we have shown here—very well contribute to the elucidation of structure–function relationships and a better understanding of ENaC function.

Materials and methods

Site-directed mutagenesis

Point mutations were introduced into α, β and γrENaC by recombinant PCR using *Pfu* DNA polymerase (Stratagene). Briefly, two fragments were amplified with primers containing the mutation in a short overlapping region, joined by recombinant PCR, digested by appropriate restriction endonucleases (αENaC: *Eco*RI–*Xba*I, βENaC: *Apa*I, γENaC: *Pst*I) and ligated into the corresponding rat ENaC cDNA in the vector pSD5. For αENaC, a cDNA clone was used in which the *Eco*RI site in the insert had been eliminated without changing the amino acid sequence, and for γENaC one in which the *Pst*I site in the vector had been eliminated. PCR-derived fragments were entirely sequenced.

Some of the ENaC subunits used for co-immunoprecipitations and the binding assay (see below) were epitope tagged. α, β and γrENaC were tagged with the FLAG reporter octapeptide (DYKDDDDK) which is recognized by the anti-FLAG M_2 IgG_1 mouse monoclonal antibody (International Biotechnology). The FLAG epitope was introduced into the proximal part of the extracellular loop of ENaC subunits (Canessa *et al.*, 1994a; Renard *et al.*, 1994; Snyder *et al.*, 1994) using recombinant PCR. In αrENaC, the FLAG sequence replaced the sequence T194RQAGARR201, in βrENaC it was inserted between T137 and S138, and in γrENaC it replaced the sequence M142PSTLEGT149.

Expression of ENaC in X.laevis oocytes

Capped cRNA was synthesized by SP6 RNA polymerase from wild-type and mutant α, β and γENaC cDNA which had been linearized by *Bgl*II (α and βrENaC) or *Pvu*II (γrENaC). Equal saturating amounts of each subunit (3 ng of cRNA of each subunit) were injected into stage V–VI oocytes of *X.laevis*. Oocytes were either kept in modified Barth's saline (MBS: 88 mM NaCl, 1.0 mM KCl, 2.4 mM $NaHCO_3$, 0.41 mM $CaCl_2$, 0.33 mM $CaNO_3$, 0.82 mM $MgSO_4$, 10 mM HEPES, pH 7.2) and the macroscopic amiloride-sensitive sodium current (I_{Na}) was determined 24 h after injection or in low-sodium MBS (10 mM NaCl, 90 mM NMDG-Cl, 5 mM KCl, 0.41 mM $CaCl_2$, 0.33 mM $CaNO_3$, 0.82 mM $MgSO_4$) and I_{Na} was determined 48 h after injection. I_{Na} was determined using two-electrode voltage-clamp as described elsewhere (Canessa *et al.*, 1993) in the presence of 5 μM amiloride.

Results are reported as means ± SEM and represent the mean of *n* independent experiments in which the average amiloride-sensitive sodium current I_{Na} was measured for 4–8 individual oocytes originating from the same frog. Data on graphs represent the percentage of I_{Na} measured for mutant channels relative to I_{Na} of wild-type channels. Statistical analysis was done with the unpaired *t*-test.

Co-immunoprecipitation

Xenopus oocytes injected with cRNAs coding for wild-type or mutant α, β and γENaC were incubated for 14 h in MBS supplemented with 1.0 mCi/ml of [^{35}S]methionine. Either β or γ subunits were tagged with the FLAG epitope. Oocytes containing no tagged subunit served as a negative control. Microsomal membranes were prepared as described (Geering *et al.*, 1989), microsomal proteins solubilized in a digitonin washing buffer [DWB: 20 mM Tris pH 7.6, 100 mM NaCl, 0.5% digitonin, 1 mM phenylmethylsulfonyl fluoride (PMSF), Leupeptin, Antipain, Pepstatin A (Sigma) (LAP)], and the incorporated radioactivity determined. Equal amounts of counts were supplemented to a final concentration of 2% bovine serum albumin and 2 mM PMSF, and ENaC subunits precipitated using the anti-FLAG M_2 IgG_1 monoclonal antibody o/n at 4°C. The immunoprecipitates were recovered with protein G–Sepharose, washed four times with DWB and twice with DWB not containing digitonin, and separated on a 5–8% gradient SDS–polyacrylamide gel. The gel was exposed for 4–7 days on Kodak XS film.

Binding assay

Anti-FLAG M_2 IgG_1 monoclonal antibody was iodinated using the Iodo-Beads Iodination reagent (Pierce) and carrier-free [^{125}I]Na (Amersham) according to the Pierce protocol. Iodinated antibody had a specific activity of $5–20\times10^{17}$ c.p.m./mol and was utilized during 2 months after the synthesis. Binding of the iodinated antibody to oocytes expressing the FLAG-containing ENaC subunits was determined 20–24 h after the cRNA injection. Twelve oocytes in each experimental group were transferred into a 2 ml Eppendorf tube containing MBS solution supplemented with 10% heat-inactivated calf serum and incubated for 30 min on ice. The binding was started by the addition of 12 nM (K_d = 3 nM) of the iodinated antibody in a final volume of 100 μl. After 1 h incubation on ice, the oocytes were washed eight times with 1 ml of MBS solution supplemented with 5% calf serum and then transferred individually into tubes containing 250 μl of MBS. The samples were counted and the same oocytes utilized for two-electrode voltage-clamp studies. Non-specific binding was determined on oocytes injected with untagged ENaC subunits.

Results are reported as means ± SEM and represent the mean of six independent experiments in which the average anti-FLAG IgG binding and the average amiloride-sensitive sodium current I_{Na} were measured for 5–8 individual oocytes originating from the same frog. Data on graphs represent the percentage of IgG bound and of I_{Na} measured for mutant channels relative to the IgG bound and of I_{Na} of wild-type channels. Statistical analysis was done with the unpaired *t*-test.

Patch–clamp experiments

Channel recordings were obtained from defolliculated oocytes in the cell-attached configuration. Pipet solution contained in mM: 110 NaCl or 110 LiCl; 2.5 KCl; 1.8 $CaCl_2$; 10 HEPES–NaOH pH 7.2; bath solution was identical to pipet solution except that 110 mM KCl replaced NaCl. Data were sampled at 2 kHz and filtered at 200–500 Hz for analysis. Single channel conductance was obtained from amplitude histograms of open state current of at least 50 transitions. The open state probability (P_o) was determined from 4 to 15 min segments of digitized single channel data using a 50% threshold criterion to distinguish open from closed states.

Acknowledgements

We thank Nicole Skarda-Coderey for secretarial assistance and Hans-Peter Gaeggeler for technical help. This work was supported by grants from the Swiss National Fund for Scientific Research to B.C.R. (# 31-43384.95) and to L.S. (# 31-39435.93). R.P.L. is an investigator of the Howard Hughes Medical Institute.

References

Canessa,C.M., Horisberger,J.D. and Rossier,B.C. (1993) Epithelial sodium channel related to proteins involved in neurodegeneration. *Nature*, **361**, 467–470.

Canessa,C.M., Merillat,A.-M. and Rossier,B.C. (1994a) Membrane topology of the epithelial sodium channel in intact cells. *Am. J. Physiol.*, **267**, C1682–C1690.

Canessa,C.M., Schild,L., Buell,G., Thorens,B., Gautschi,I., Horisberger,J.-D. and Rossier,B.C. (1994b) Amiloride-sensitive epithelial Na^+ channel is made of three homologous subunits. *Nature*, **367**, 463–467.

Chalfie,M. and Wolinsky,E. (1990) The identification and suppression of inherited neurodegeneration in *Caernorhabditis elegans*. *Nature*, **345**, 410–416.

Chalfie,M., Driscoll,M. and Huang,M.X. (1993) Degenerin similarities. *Nature*, **361**, 504.

Chang,S.S. *et al.* (1996) Mutations in subunits of the epithelial sodium channel cause salt wasting with hyperkalaemic acidosis, pseudohypoaldosteronism type 1. *Nature Genet.*, **12**, 248–253.

Duc,C., Farman,N., Canessa,C.M., Bonvalet,J.-P. and Rossier,B.C. (1994) Cell-specific expression of epithelial sodium channel α, β, and γ subunits in aldosterone-responsive epithelia from the rat: localization

by *in situ* hybridization and immunocytochemistry. *J. Cell Biol.*, **127**, 1907–1921.
Firsov,D., Schild,L., Gautschi,I., Mérillat,A.-M., Schneeberger,E. and Rossier,B.C. (1996) Cell surface expression of the epithelial sodium channel and a mutant causing Liddle syndrome: A quantitative approach. *Proc. Natl Acad. Sci. USA*, **93**, 15370–15375.
Geering,K., Theulaz,I., Verrey,F., Hauptle,M.T. and Rossier,B.C. (1989) A role for the β-subunit in the expression of functional Na,K-ATPase in *Xenopus* oocytes. *Am. J. Physiol*., **257**, C851–C858.
Hansson,J.H. *et al*. (1995) Hypertension caused by a truncated epithelial sodium channel γ subunit: genetic heterogeneity of Liddle syndrome. *Nature Genet.*, **11**, 76–82.
Huang,M. and Chalfie,M. (1994) Gene interactions affecting mechanosensory transduction in *Caenorhabditis elegans*. *Nature*, **367**, 467–470.
Kemendy,A.E., Kleyman,T.R. and Eaton,D.C. (1992) Aldosterone alters the open probability of amiloride-blockable sodium channels in A6 epithelia. *Am. J. Physiol*., **263**, C825–C837.
Li,X.-J., Xu,R.-H., Guggino,W.B. and Snyder,S.H. (1995) Alternatively spliced forms of the α subunit of the epithelial sodium channel: distinct sites for amiloride binding and channel pore. *Mol. Pharmacol.*, **47**, 1133–1140.
McDonald,F.J., Snyder,P.M., McCray,P.B. and Welsh,M.J. (1994) Cloning, expression, and tissue distribution of a human amiloride-sensitive Na^+ channel. *Am. J. Physiol.*, **266**, L728–L734.
McDonald,F.J., Price,M.P., Snyder,P.M. and Welsh,M.J. (1995) Cloning and expression of the β- and γ-subunits of the human epithelial sodium channel. *Am. J. Physiol.*, **268**, C1157–C1163.
Palmer,L.G. and Frindt,G. (1986) Amiloride-sensitive Na^+ channels from the apical membrane of the rat cortical collecting tubule. *Proc. Natl Acad. Sci. USA*, **83**, 2767–2770.
Palmer,L.G. and Frindt,G. (1996) Gating of Na channels in the rat cortical collecting tubule: effects of voltage and membrane stretch. *J. Gen. Physiol.*, **107**, 35–45.
Puoti,A., May,A., Canessa,C.M., Horisberger,J.-D., Schild,L. and Rossier,B.C. (1995) The highly selective low-conductance epithelial Na channel of *Xenopus laevis* A6 kidney cells. *Am. J. Physiol.*, **38**, C188–C197.
Renard,S., Lingueglia,E., Voilley,N., Lazdunski,M. and Barbry,P. (1994) Biochemical analysis of the membrane topology of the amiloride-sensitive Na^+ channel. *J. Biol. Chem.*, **269**, 12981–12986.
Rossier,B.C. and Palmer,L.G. (1992) Mechanisms of aldosterone action on sodium and potassium transport. In Seldin,D.W. and Giebiesch,G. (eds), *The Kidney, Physiology and Pathophysiology.* Raven Press, New York, pp. 1373–1409.
Rossier,B.C., Canessa,C.M., Schild,L. and Horisberger,J.-D. (1994) Epithelial sodium channels. *Curr. Opin. Nephrol. Hypertension*, **3**, 487–496.
Schild,L., Canessa,C.M., Shimkets,R.A., Gautschi,I., Lifton,R.P. and Rossier,B.C. (1995) A mutation in the epithelial sodium channel causing Liddle disease increases channel activity in the *Xenopus laevis* oocyte expression system. *Proc. Natl Acad. Sci. USA*, **92**, 5699–5703.
Shimkets,R.A. *et al*. (1994) Liddle's syndrome: heritable human hypertension caused by mutations in the β subunit of the epithelial sodium channel. *Cell*, **79**, 407–414.
Snyder,P.M., McDonald,F.J., Stokes,J.B. and Welsh,M.J. (1994) Membrane topology of the amiloride-sensitive epithelial sodium channel. *J. Biol. Chem*., **269**, 24379–24383.
Snyder,P.M., Price,M.P., McDonald,F.J., Adams,C.M., Volk,K.A., Zeiher,B.G., Stokes,J.B. and Welsh,M.J. (1995) Mechanism by which Liddle's syndrome mutations increase activity of a human epithelial Na^+ channel. *Cell*, **83**, 969–978.
Strautnieks,S.S., Thompson,R.J., Gardiner,R.M. and Chung,E. (1996) A novel splice-site mutation in the γ subunit of the epithelial sodium channel gene in three pseudohypoaldosteronism type 1 families. *Nature Genet.*, **13**, 248–250.
Tamura,H., Schild,L., Enomoto,N., Matsui,N., Marumo,F., Rossier,B.C. and Sasaki,S. (1996) Liddle disease caused by a missense mutation of β subunit of the epithelial sodium channel gene. *J. Clin. Invest.*, **97**, 1780–1784.
Waldmann,R., Champigny,G., Bassilana,F., Voilley,N. and Lazdunski,M. (1995) Molecular cloning and functional expression of a novel amiloride-sensitive Na^+ channel. *J. Biol. Chem.*, **270**, 27411–27414.

Received on August 8, 1996; revised on November 5, 1996